

Solid Core Photonic Crystal Fiber for Dispersion tailoring in Optical Tele Communication systems

G. Latha

Department of Physics, AVIT, Vinayaka Mission's Research Foundation, Chennai, India, 603104

Abstract. The studies have been carried out on the viability in realizing fully infiltrated solid core photonic crystal fiber based dispersion compensating fiber with suitable high index infiltrate and tapered solid core large mode area fiber for optical communication networks in telecommunication band. The commercial fiber LMA-20 can be made to stretch negative dispersion by suitable fluid infiltration in all air holes of fiber cladding hexagonal structure and can be used as an alternative of existing dispersion compensators (PCFs with low pitch values).

Keywords: Holy fiber, Dispersion compensating fiber (DCF), High index fluids, Tapered PCF

* Correspondence Author, E-mail: latha.physics@avit.ac.in

1 Introduction

Dynamic bandwidth provisioning requirement in today's elastic bandwidth optical networks require programmable dispersion controls. The major focus of the work addresses the issue of how to arrive at a design for programmable dispersion compensation using commercially available solid core photonic crystal fibers (SCPCFs) without devising to design specialty fibers for this. Selective fluid infiltration in the micro-structured cladding of SCPCFs or SCPCF tapers have been used to modify its dispersion properties to meet some key requirements in telecommunication systems as dispersion shifted fibers (DSFs) or dispersion compensating fibers (DCFs)[10,11]. This effort is aimed to study the changes in the dispersion properties of SCPCF with respect to the change in RI of infiltrates which has been fully infiltrated in an LMA-20 SCPCF and therefore to arrive at a simple methodology to predict the dispersion that can be achieved for the design of dispersion controllers for a given frequency band.

2 Modeling methodology

2.1 FEM modeling

FEM modeling allows one to extract all critical metrics and the transmission characteristics of the PCF. COMSOL Multiphysics, version 4.4a with the RF module, is employed to extract effective index of the fundamental modes and the dispersion values of air-filled and high-index fluid filled LMA-20 PCFs are modeled. The agreement of the FEM results to the predictions from transfer matrix method (TMM) shows that this can serve as an initial guideline for selecting regions of specific interest for developing applications [6].

2.1 TMM modeling of LMAPCF

TMM technique used to model the propagation of the electromagnetic field through a SCPCF comprising of air or fluid filled holes in a host matrix of silica [5]. Fig.1 depicts the schematic of the cross-section of the LMA-20 SCPCF (ThorLabs). This modeling is employed to illustrate the electromagnetic field propagation through PCF comprising of air or fluid filled holes in silica background. It can be seen that along all the axes passing through the opposite vertices (Γ X, Γ -K directions) of the central innermost hexagonal represented by orange dashed lines, the periodic pattern consists of six bilayers of silica and air on either side of central defect region (core) summing up to a total of 25 layers. The representative 1D photonic band gap (PBG) structure for these directions is represented at the bottom of Fig.1. Here dx is the thickness of the pure silica layer, h the dimension of micro-hole and dxd , the dimension of the defect layer which is central silica core. The other set of distinct periodic structures are the ones along the centre of the hexagonal sides of the core region (Γ -M direction) which is depicted separately on the left side of the cross-sectional image in Fig.1. These have 25 layers along X-axis and 13 layers along Y-

axis, where the relative permittivity $\epsilon(z)$ and relative permeability $\mu(z)$ can take any real value but are constant within each layer. The omnidirectional band gap of the PCF can be obtained from a super positioning of the band gap of these two structures. The band gap will pertain to bands where the transmission from core region to the right through this structure is low.

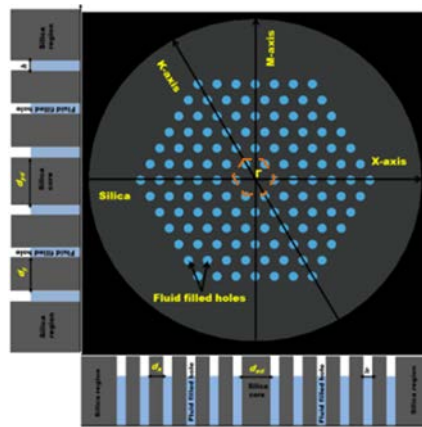


Fig.1 Cross-section of LMA -20 PCF

The stopbands in the transfer function of these PBGs are the frequencies that are not coupled out through the microstructured cladding and are hence the frequencies that are confined in the core of the PCF. The influence of fluid infiltrated either fully or selectively, in the microstructure can be easily taken into account, as the change in the refractive index of the fluid filling the microhole changes the propagation and interface matrices M_p and M_I accordingly. The transmission characteristics of representative 1D PBGs of LMA-20SCPCF have been numerically simulated using MATLAB with dispersion of silica accounted for using Sellmeier's equation with appropriate coefficients [6]. In the TMM simulation implemented in MATLAB, dispersion of silica is taken into account through Sellmeier's equation which calculates n_{silica} with constants as depicted in equation (1).

$$n_{silica}(\lambda) = \sqrt{1 + \frac{(b1*(\lambda*1e6)^2)}{((\lambda*1e6)^2)-c1^2} + \frac{(b2*(\lambda*1e6)^2)}{((\lambda*1e6)^2)-c2^2} + \frac{(b3*(\lambda*1e6)^2)}{((\lambda*1e6)^2)-c3^2}} \tag{1}$$

Where $b_1=0.6961663$; $c_1=0.0684043$; $b_2=0.4079426$; $c_2=0.1162414$; $b_3=0.8974794$; $c_3=9.896161$ and wavelength λ is in m.

Fig.2 shows an enlarged view of the transmission spectrum close to 1550 nm showing that 1.51-1.53 the losses due to transmission through the microstructured cladding is more and core guidance is comparatively much better in the 1532 nm to 1552 nm bands. A comparison with the TMM simulation results in the wavelength range from 1500 nm-1600 nm shows that at n_{fluid} values where the FEM predicts a complex effective index, TMM also predicts high transmission losses.

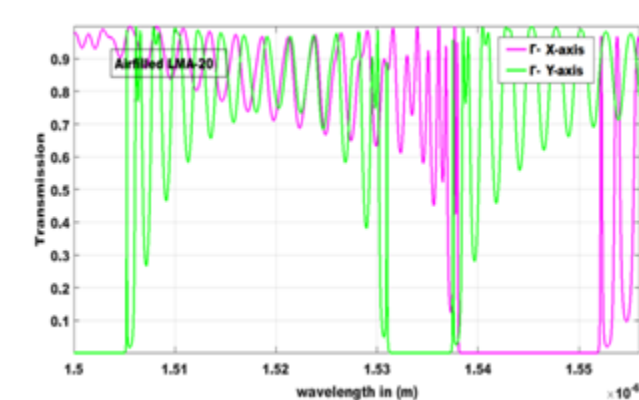


Fig.2 Transmission spectra of air-filled LMA-20 in the 1500nm-1560nm region

For n_{fluid} values at which transmission losses are less than 10%, mode patterns obtained from FEM confirms the strong confinement in the silica core of the PCF. The agreement of the FEM results to the predictions from TMM shows that TMM modeling can serve as an initial guideline for selecting regions of specific interest for developing applications.

3 Dispersion tailoring

Geometrical changes to the PCF can give moderate negative dispersion over a larger frequency band to compensate for the positive dispersion in conventional single mode fibers. Moderate negative dispersion say -100ps/nm/km implies 150m of PCF for compensation of

dispersion of 15ps from an SMF of length 1km. This could at the most be a viable option for dispersion compensation in LANs, but cannot be a solution for larger networks that has to compensate for dispersion for 100kms. As per literature reports, waveguide modifications through full or selective infiltration of the microholes of the SCPCF, on the other hand, can achieve very high negative dispersion in a limited frequency band which implies few centimeters of PCF lengths, minimizing the loss budget.

PCF in the PBG regime can provide anomalous dispersion and since we are able to predict the PBG regime using simple TMM modeling of the PCF, our studies concentrate on how to predict the large negative dispersions of thousands of ps/nm/km that is possible by full infiltration of the microstructure using fluids with RI that ensures photonic band gap guidance in the waveband of interest. Zero dispersion shifting to longer wavelengths and low dispersion slope profiles are also possible through the appropriate selection of infiltrate. For these studies, we concentrate on achieving negative dispersion in the third telecommunication window though the method can be extended to other regions too. The scheme that is going to be investigated is as shown in Fig.3.

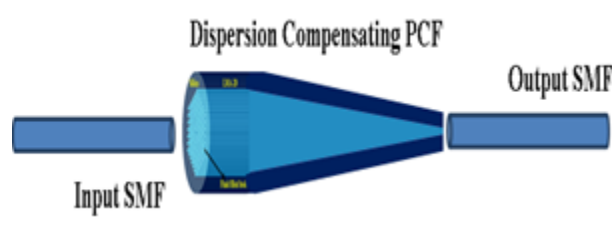


Fig.3 Schematic of infiltrated DC PCF

3.1 Dispersion in air filled LMA-20 SCPCF

The chromatic dispersion D_{PCF} is calculated from the variation of n_{eff} values with wavelength, using the standard expression reproduced below as equation (2).

$$D_{PCF} = -\left(\frac{\lambda}{c}\right)\left(\frac{\partial^2 n}{\partial \lambda^2}\right) \quad (2)$$

Dispersion analysis is performed from n_{eff} values estimated using FEM and also from analytical studies for LMA-20. Generally, the dispersion for air-filled LMA fibers is positive in the order of 50.0ps/nm/km as specified by the LMA-20 datasheets. The maximum dispersion calculated using FEM (50.34ps/nm/km) is also in the same range as specified in the datasheet. However, dispersion curve calculated using FEM shows a fine structure in the dispersion values which can be correlated to the transmission spectrum of the microstructure obtained through TMM analysis. An expanded view of the transmission spectra through the microstructures for air-filled LMA-20 in the 1500 nm to 1600 nm is given in Fig. 4(b). When the confinement of power in the silica core in the Γ -Y PBG structure is high (i.e. transmission through the structure is nearly zero), dispersion of the confined mode is found to be minimal.

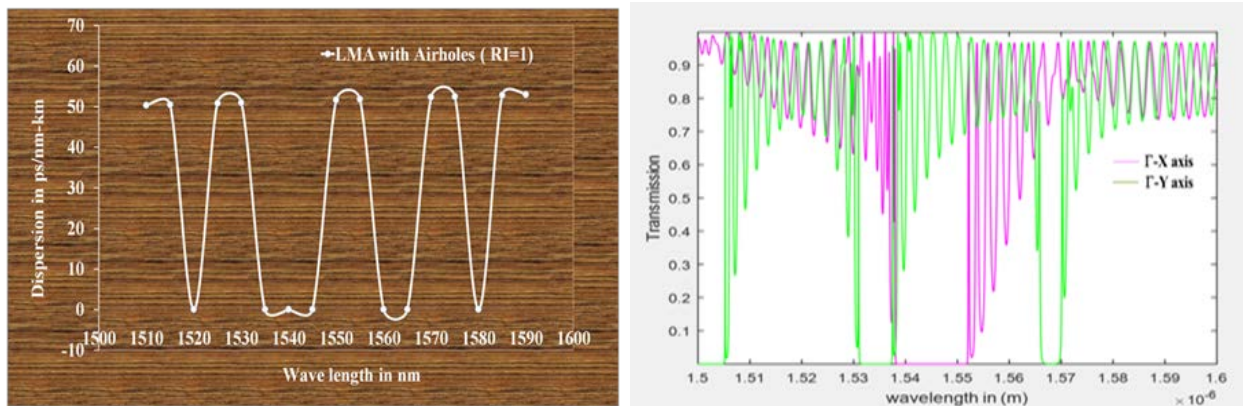


Fig. 4 (a) Dispersion of air-filled LMA-20 by FEM (b) TMM based transmission spectrum through the microstructured cladding of air filled LMA20PCF

If D_{SMF} , D_{PCF} , represents the dispersion in ps/nm.km for standard SM telecommunication fibers and PCFs respectively and L_{SMF} and L_{PCF} the corresponding lengths of fibers used, then for effective dispersion compensation for a length of a single mode fiber L_{SMF} ,

$$-D_{SMF}(\lambda).L_{SMF} = D_{PCF}(\lambda).L_{PCF} \quad (3)$$

In other words, the total dispersion of SMF fiber of length L_{SMF} should be equal in magnitude but opposite in sign to the total dispersion offered by the PCF of length L_{PCF} . As SMFs and PCFs generally have positive dispersion in the 1500nm-1600nm telecommunication window, the PCF has to be tailored (through modification of its waveguide) to give a negative dispersion. As losses of PCFs are generally higher than that of SMF, the length of PCF used for compensation should be less and this necessitates large negative values of D_{PCF} . For flat dispersion compensation in the wavelength band of interest, the relationship given in equation (3) has to be satisfied for all wavelengths within the band of interest.

3.2 Infiltrated LMA SCPCF based dispersion control

In a solid core PCF, the dispersion characteristics can be altered by varying its structural parameters and by mode modulations through infiltration. Air inclusions in LMA fiber structure can be easily filled with fluids. The previous studies reported here in this thesis has shown that if materials with RI in the range of 1.5-1.9 are infiltrated into the micro-holes in the cladding of the SCPCF, the index difference between micro-structured cladding and core is high enough to confine the guided mode into the core by photonic band gap guidance.

When the RI of the fluid (n_{fluid}) infiltrated into the micro-holes of the cladding has an index of 1.7, the index contrast between the silica core and that of the cladding $n_{eff_{clad}}$ is approximately -0.065. The mode pattern is Gaussian and predominantly confined to the core. The

dispersion estimated from FEM analysis and the transmission through the microstructure using TMM is depicted in Fig. 5(b).

3.3 Tapering of LMA-20 SCPCF

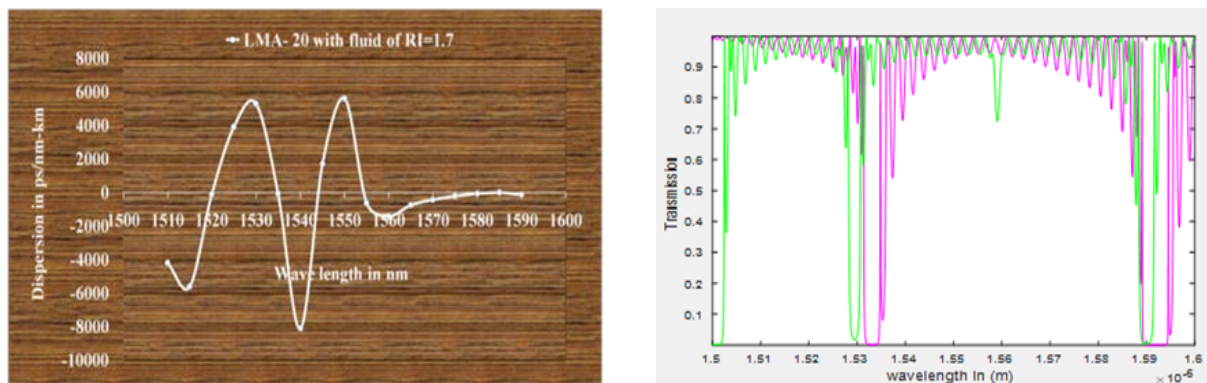


Fig. 5 (a) Dispersion profile (b) transmission through microstructure for LMA-20 infiltrated with fluid of RI =1.7

For infiltrate fluids of index higher than silica, good confinement (transmission through cladding microstructure less than 30%) in the Γ -Y Axis based on TMM analysis provides negative dispersion slopes and when confinement in both axes is high (i.e. they are resonant frequencies of the central defect region, transmission through cladding microstructure less than 10%) high negative dispersion (10^3 ps/nm.km) can be achieved. Comparison of TMM and FEM results in Table1 shows that TMM studies can predict wavelength regions where negative dispersions can be observed using fluid infiltration.

Table 1 Negative dispersion analysis in infiltrated LMA-20

Fluid RI	Transmission along Γ -X Axis (TMM)	Transmission along Γ -Y Axis (TMM)	D in (ps/nm.km) (FEM)
1.7 (Near PBG region)	> 0.9	> 0.9	Positive (5×10^3 to 6×10^3)
	~ 0.6	~ 0.3	Nearly zero dispersion
	< 0.1	< 0.1	Highly Negative (-8×10^3)
1.9	> 0.9	> 0.9	Positive (1.4×10^3)

(PBG region)	~ 0.7	~ 0.7	Nearly Zero dispersion
	> 0.3	< 0.1	Highly Negative (-3.5×10^3)

When the fiber is tapered, the core diameter decreases along the propagation direction and if tapering is done without collapse of the holes by manipulating adequate air pressure in the micro holes [1,9], the transverse cross-sectional geometry gets preserved though dimensions scale down. If hole diameter of LMA-20 is reduced to $1/10^{\text{th}}$ of its original (i.e. to $0.64 \mu\text{m}$), and pitch is also reduced symmetrically to $1/10^{\text{th}}$ (to $1.32 \mu\text{m}$), a core diameter reduces to $2 \mu\text{m}$ through tapering. The mode pattern of the tapered LMA-20 also shows low birefringence introduced by tapering as shown in Fig.6. The dispersion calculated by FEM is mostly negative over the whole C-band and has magnitudes between -50 to -404 ps/nm-km whereas FDTD studies show a smaller range of variation of dispersion from -100 to -204 ps/nm/km . FEM simulation shows negative dispersion values as shown in Fig .6 (-100 to -150 ps/nm-km). This shows that tapering the LMA-20 can ensure negative dispersion for the C-band but would need 1.5m of tapered fiber to compensate for the dispersion of 1km SM fiber. Tapering can also be used as a 3D beam modifier reducing the MFD from 20 microns to 2.6 microns with fixed pre-compensation in the C-band. Infiltration of tapered fibers gives positive dispersion and is therefore not considered here.

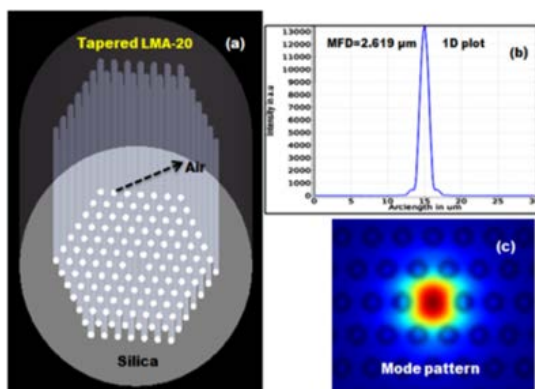


Fig. 6 Air filled LMA-20 Taper 3D view
(b) Intensity profile (c) Mode pattern

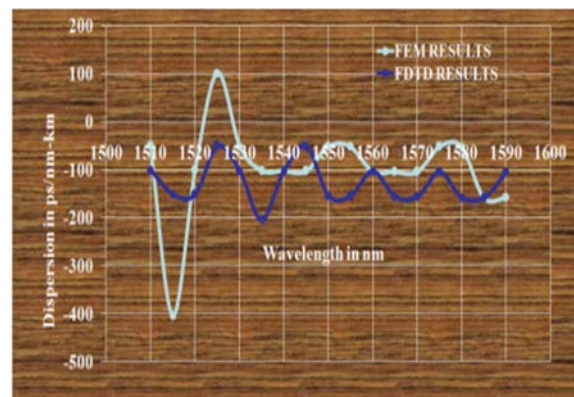


Fig. 7 Dispersion characteristics of air filled LMA Taper by FEM and FDTD

This result shows that tapering the LMA-20 can ensure negative dispersion for the C-band but would need 1.5m of tapered fiber to compensate for the dispersion of 1km SMF. Tapering can also be used as a 3D beam modifier reducing the MFD from 20 microns to 2.6 microns with fixed pre-compensation in the C-band. Infiltration of tapered fibers gives positive dispersion and is therefore not considered here.

4 Tunable infiltrated PCF based dispersion compensator

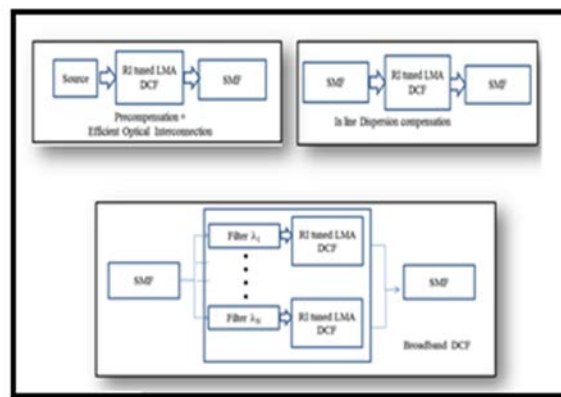


Fig.8 Schemes for employing SCPCFs as DCF units

An inline dispersion compensator can be configured using infiltrated PCFs. Thermal or electro-optic tuning of the infiltrate RI can change the dispersion characteristics of the PCF. For high negative dispersion compensation at spot wavelengths, the signal wavelength after filtering through a 10nm filter centred at this wavelength can be passed through a short section of photonic band gap (PBG) guided PCF. With a PCF optimized to provide -8000ps/nm/km, a length of 1m can compensate for dispersion accrued by 533m of SMF. RI of infiltrate can be tuned using EO effect if the fluid infiltrated is in the form of an EO polymer or melt grown crystal or through thermal tuning. Both will be in solid form after setting and will not require any sealant to hold them in. This can then become a programmable dispersion compensating fiber

(DCF). The block diagrams of how they can be employed as pre-compensator, inline compensator or a broadband compensator are shown in Fig.8 given below.

5 Conclusion

Effect of fluid infiltration and tapering of LMAPCFs on its dispersion profiles have been explored through simulations. Broadband low negative dispersion of the order of -100ps/nm.km can be achieved through tapering. High negative dispersion at spot wavelengths are achievable for specific fluid/solid refractive indices s in the PBG guidance regime in an infiltrated large mode area solid core photonic crystal fibers. Wavelength bands where high negative dispersion can be achieved for a particular refractive index of the infiltrate can be predicted from knowledge of the stop bands of the one dimensional photonic band gap structure constitutes the PCF. Refractive index tuning based tunable PCF based DCFs have been proposed for LANs and MANs.

References

1. Birks, TA, Knight, JC & Russell, PStJ, "Endlessly single-mode photonic crystal fiber", Optics Letters, vol. **22**, 961-963,1997.
2. Buczynski, R, "Photonic Crystal Fibers", Acta Physica Polonica Series A, **106**(2), 141-168,2004.
3. P. S. J. Russell, "Photonic-Crystal Fibers," J. Light wave Technology. **24**(12), 4729–4749, 2006.
4. G.P.Agarwal, "Fiber optic communication systems, Wiley-Inter science, 1997.
5. Sophocles J. Orfanidis, "Electromagnetic Waves and Antennas"
<http://www.ece.rutgers.edu/~orfanidi/ewa/>,2002.
6. Latha, G & Prita Nair , "Commercial Solid Core Photonic Crystal Fibers for Sensing Applications", Proceedings of the COMSOL International Conference, Bangalore, India, 4-5 November,2014.

7. Dehghan, F, Ebnali-Heidari, M & Shi, Q, "Dispersion engineering of photonic crystal fibers using fluidic infiltration technology", IEEE, 2010.
8. Chen, Z, Xiaoming Xi, Jing, ZW & Jiang, ZF, "Low-Loss Fusion Splicing Photonic Crystal Fibers and Double Cladding Fibers by Controlled Hole Collapse and Tapering", Journal of Light wave Technology, **29**(24), 3744-3747, 2011.
9. Zhou H, Chen Z, Xi X, Hou J& Chen J, "Effective way of reducing coupling loss between rectangular micro-waveguide and fiber", Applied optics, **51**(3), 390-393, 2012.
10. Partha Sona Maji, Partha Roy Chaudhuri "A New Design of Ultra-Flattened Near-zero Dispersion PCF Using Selectively Liquid Infiltration" Photonics and Optoelectronics (P&O), **2**(2), April, 2013.
11. Redwan Ahmad, A. H. Siddique" Design of a Photonic Crystal Fiber for Dispersion Compensation over Telecommunication Bands" International Conference on Electrical Information and Communication Technology (EICT), 2013.
12. P. Marca, A. Gieraja, M. Murawska, "Thermo - optic properties of Co Nano fluid filled microstructured fiber" proceedings of SPIE - the international society for optical engineering • may 2013.
13. Sourabh Roy, KajalMondal & Partha Roy Chaudhuri, "Effect of tapering realistic photonic crystal fiber in tailoring birefringence and dispersion properties", (ICOP) International conference on optics and photonics, 2009.
14. Maji, PS & Choudhary, PR, "Circular Photonic Crystal Fibers: Numerical Analysis of Chromatic Dispersion and Dispersion Losses", ISRN Optics, vol. 13, Article ID 986924, 1-9,2013.
15. E. C. Magi, P. Stein vurzel, and B.J. Eggleton2004, "Tapered Photonic Crystal Fibers", OPTICS EXPRESS,vol.**15**, 776.
16. H.C. Nguyen et al. "Tapered photonic crystal fibers: properties, characterization and applications," Appl. Phys. B 81, 377–387, 2005.
17. Kuhlmeiy, BT, Eggleton, BJ & Darran K. C. Wu, "Fluid-Filled Solid-Core Photonic Bandgap Fibers", Journal of Light wave Technology, **27**(11), June 1, pg. 1617-1629,2009.